high-speed digital networks. Over the past few years, he also has consulted with several companies in the areas of digital control systems, X-ray tomography, and doppler ultrasound.

Mr. Slaney is a member of ACM and Eta Kappa Nu.

✤

**Avinash C. Kak** (M'71) is currently a Professor of Electrical Engineering at Purdue University, West Lafayette, IN. His current research interests are in computed imaging, image processing, and artificial intelligence. He has coauthored *Digital Picture Processing*, vols. 1 and 2 (New York: Academic), a second edition of which was published in 1983. He is an Associate Editor of *Computer Vision, Graphics and Image Processing* (New York: Academic), and *Ultrasonic Imaging* (New York: Academic). He was also a Guest Editor of the February 1981 Special Issue on Computed Imaging of the IEEE TRANSACTIONS ON BIOMEDICAL ENGINEERING. During the last ten years, he has consulted in the areas of computed imaging for many industrial and governmental organizations.

✤

**Lawrence E. Larsen** (M'81–SM'82) attended and received the M.D. degree magna cum laude from the University of Colorado, Fort Collins, in 1968. He was awarded an NIH postdoctoral fellowship in biophysics at UCLA for the period 1968–1970.

He then served in the United States Army as a Research Physiologist in the Department of Microwave Research at the Walter Reed Army Institute of Research during 1970–1973. From 1973 to 1975, he accepted a faculty appointment in the Radiology Department at the Baylor College of Medicine in Houston, TX, where he taught physiology and computer sciences. In 1975, he returned to the Walter Reed Army Institute of Research as the Associate Chief of Microwave Research. He was appointed the Department Chief in 1977 and presently serves in that role with the rank of Colonel, Medical Corps. He holds several patents.

# Hyperthermia and Inhomogeneous Tissue Effects Using an Annular Phased Array

PAUL F. TURNER

*Abstract*—**A regional hyperthermia Annular Phased Array (APA) applicator is described, and examples of its various heating patterns, obtained by scanning the electric fields with a small E-field sensor, are illustrated. Also shown are the effects of different frequencies of an elliptical phantom cylinder having a 1-cm-thick artificial fat wall and the general dimensions of the human trunk. These studies show the APA's ability to achieve uniform heating at lower frequencies (below 70 MHz) or to focus central heating at moderately higher frequencies (above 70 MHz). The influence of human anatomical contours in altering heating patterns is discussed using results obtained with a female mannequin having a thin latex shell filled with tissue-equivalent phantom. Field perturbations caused by internally embedded low-dielectric structures are presented, showing the localized effects of small objects whose surfaces are perpendicular to the electric field.**

## I. INTRODUCTION

ELECTROMAGNETIC (EM) hyperthermia has been clinically tested, for the most part, with superficial tumors in which the response is easily measured. Results obtained in these clinical trials corroborate findings from earlier *in vivo* and *in vitro* experiments that show this technique to be capable of selectively treating cancerous tumors. Much of the real potential of hyperthermia, however, lies in its ability to treat deep-seated localized tumors for which surgical removal is not a feasible solution. Such tumors have consistently presented one of the most difficult challenges facing both oncologists and technical researchers.

In response to this need, BSD Medical Corporation has developed an EM Annular Phased Array, or APA (patent pending), shown in Fig. 1, which has undergone testing since 1979 and which, during that time, has been shown to be capable of transmitting heating power directly to central body tissues [1]. The interaction of the human body and the EM field generated by the APA has been studied with phantom models [2], anesthetized laboratory animals [1], [3], and terminally ill human cancer patients [4], [5]. Results obtained in these trials show that deep regional hyperthermia is not only possible, but effective in controlling solid tumors in the center of the body. (Actual clinical application of this method is still restricted, primarily

Manuscript received October 12, 1983; revised March 8, 1984.

The author is with BSD Medical Corporation, 420 Chipeta Way, Suite 220, Salt Lake City, UT 84108.

0018-9480/84/0800-0874$01.00 ©1984 IEEE

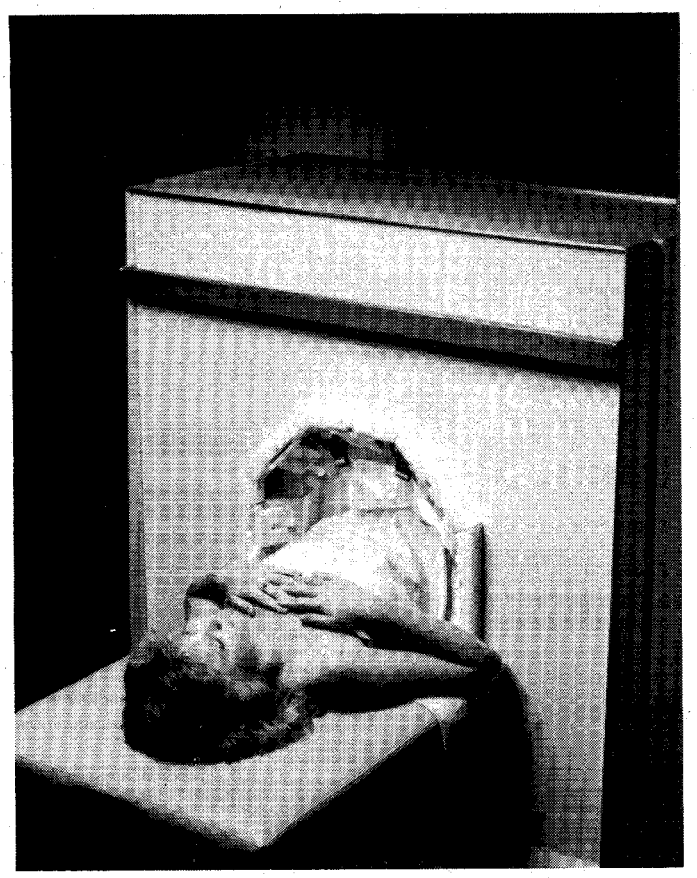

Fig. 1. Photograph of Annular Phased Array clinical setup.

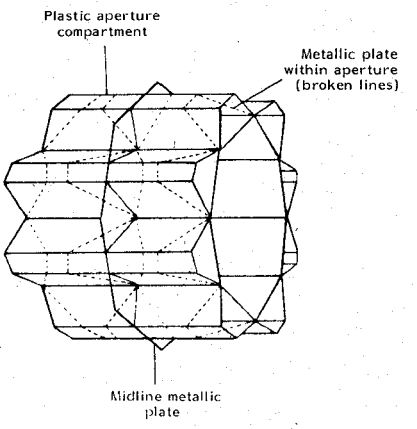


Fig. 2. Annular Phased Array internal aperture configuration (previously published) [2].

because of the numerous and complex problems which typically attend advanced cancer patients.) Steering of the heating pattern to heat the target tissue more selectively has also been demonstrated in cylindrical phantoms, but this has not been used extensively in clinical practice.

Two-dimensional numerical models have been developed which use a CAT scan image to identify the various tissues within the body and the two-dimensional cross-section effect of these tissues on the heating pattern. Data obtained from this technique agree well with phantom and animal test results, and are qualitatively consistent with temperature patterns observed in clinical trials [6].

Another recent enhancement of the APA deep-heating technique is the E-field probe, which is placed along the surface of the patient's body within the heating field. The external EM fields along the body surface have been found to correlate well with superficial heating fields, typically within 10 percent, and qualitatively with the deep-heating patterns as well. When several of these are placed around the body, it is possible to make a noninvasive estimation of the deep-heating pattern balance [7].

Throughout the testing of the APA, two phenomena which can result in localized hotter regions have been observed. One of these is believed to be related to whole-body dipole resonance [8], and the other to anatomical variations which cause the conductive currents, which are more dominant [9], to densify along narrowing conductive paths. Both of these circumstances occur with the lower frequencies that are employed with the APA to obtain increased penetration and heating field size.

As has been previously reported [2], the principles of operation and design of the APA are based on a synchronous array of TEM aperture sources. The dominant electric-field vector of each is aligned with the axial center line of the annular opening, and the radiation pattern of each aperture is directed toward the axial center line. This results in a cylindrically convergent TEM field, and thus a standing wave or interference pattern, with the phase node at the center, is established within the opening of the array. When a patient's body is placed in the center of the APA and energy is coupled to it through deionized water boluses which function as a dielectric waveguide, this penetrating interference pattern is retained, but modified by the attenuation of the tissue. The result is a penetrating field which can heat, with approximate uniformity, tissues having similar RF electrical conductivities, even within a large cross-sectional diameter like that of the human body.

The data given in the present paper demonstrate the influence of several factors on the heating pattern, an understanding of which can improve clinical effectiveness of the APA, as well as other hyperthermia techniques. The interaction of EM fields with the body is a highly complex process, but application of the concepts involved may improve clinical use and aid numerical solution methods for predicting APA heat patterns by suggesting certain approximations in the solution to make the problem numerically practical for three dimensions.

## II. Materials and Methods

The APA is an array of sixteen dielectrically loaded apertures, joined in two octagonal configurations and placed side by side, as shown in Fig. 2. Each of these apertures consists of a thin-walled, horn-shaped plastic shell filled with deionized water or other low-loss, high-dielectric fluid [2]. The $20 \times 23$-cm apertures are a hybrid design based on a flared parallel-plate waveguide construction [10]. Each aperture is connected to the same power source with coax cables of equal length and power splitters. This provides the common radiation phase front at each aperture for central heating. PVC plastic boluses filled with

deionized water are located along the inner surface of the octagonal array to couple the VHF power (usually 50–110 MHz) into the patient's body. When these boluses are expanded with water, they normally are in contact with the entire aperture surface and also fill those spaces between the aperture and the tissue mass, thus acting as a dielectric waveguide.

While Annular Phased Array studies have included actual heating of phantoms, animals, and patients, the data herein reported have been obtained through monitoring of the intensity and orientation of the EM field by a small E-field probe. The completely insulated probe contains a small-signal diode with short metallic leads. This configuration forms a 1-cm-long dipole. The diode is connected to a high-impedance amplifier through two long resistive carbon/Teflon leads [2].

In APA tests, the E-field probe was calibrated in a Crawford cell where the field intensity was changed from 0.2 mW/cm$^2$ to 60 mW/cm$^2$. The curve generated under these conditions matched that produced when the probe was inserted in tissue, although the sensitivity of the probe output voltage in the phantom is 1.5 times its level in air. This curve was then used to convert the monitored voltage to field intensity. It was observed that, for power densities in air, the detected voltage changed linearly with power density between 0.2 and 3 mW/cm$^2$.

For these E-field probe tests, the APA was rotated 90° so that the central axial line of the array opening was vertically oriented, thus allowing an upright form to be filled with tissue-equivalent saline fluid and surrounded with deionized water which coupled the apertures to the saline phantom. By using clear fluids, it was possible to position the probes within the phantom with greater precision to obtain accurate field intensity patterns. The salinity of the phantom fluid was adjusted to simulate the electrical conductivity of human tissue at a level approximately two-thirds that of muscle [8]. Conductivity and permittivity of the phantom were verified by an impedance measurement technique which utilizes a capacitive holding fixture [11].

The small E-field probe was attached at various intervals to an open, thin-walled, fluid-filled plastic tube to ensure precise positioning between reference points marked along the top and bottom edges of the phantom. One measurement was obtained at each point with the probe vertically aligned along the dominant E-field; it was then horizontally positioned and maximum levels along the horizontal direction were recorded when they were over 20 percent of the vertical fields noted at the same location. In this way, the total E-field was mapped. (The horizontal fields were very small in relation to the vertical fields, except at the outer edges of the array opening along the top and bottom surface of the water bolus.)

The accuracy of E-field probe detection is affected by the media surrounding it; however, when fields in the vicinity of an interface are scanned, no significant level changes are detected, which is to be expected at the low frequencies used with the APA. This is illustrated in Fig. 3,

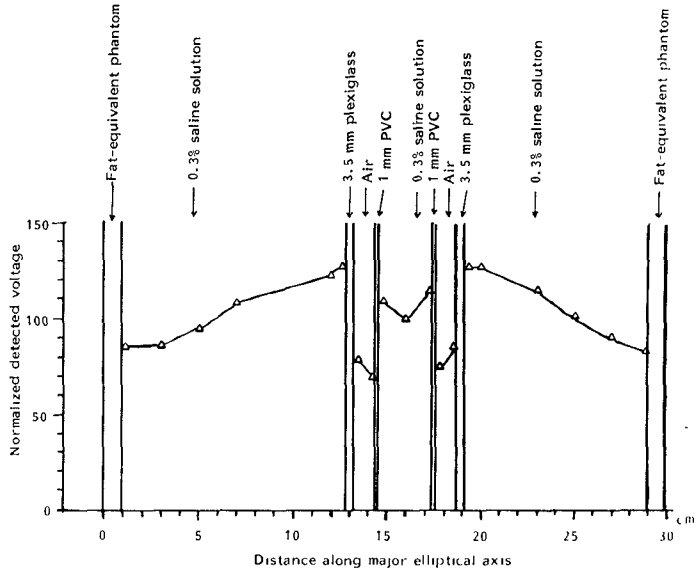


Fig. 3. E-field probe detected voltage level (normalized at center) versus position across saline solution-filled elliptical fat-equivalent phantom with centered cylinders of Plexiglas, air, PVC, and saline solution.

where the fields were scanned across the major axial cross section of a muscle-equivalent saline region inside a 1-cm-thick elliptical fat-simulating phantom, developed by A. W. Guy [12]. The inner diameter measured 28 cm along the major axis, and the minor axis was 18 cm. A long air-filled Plexiglas tube having an outer diameter of 6.2 cm and a PVC plastic tube with an inner diameter of 2.5 cm were centrally located within the elliptical phantom. The PVC tube was filled with 0.3-percent saline fluid, as was the elliptical form. The E-field probe voltage level in Fig. 3 was plotted at various positions along the central heating beam's radial line, where heating power is at a maximum. (This test was conducted within the range in which detected voltage is linear with power density.) No perturbation of the probe detection within the saline solution was observable, either at the fat phantom or the air-filled Plexiglas tube, although a change in detection sensitivity was apparent in the air-filled zone. Power levels in the central saline solution were lower, possibly because of the decoupling effect of the air. Water levels were 38 cm deep, and this may also have been a decoupling factor. The field detection levels observed in the fluid phantom are considered to be valid, even in the presence of objects having other dielectric constants.

Details of the calibration method for the E-field probes and the phantom tests are described elsewhere [2].

## III. Results

The basic power-focusing ability of the APA is illustrated in Fig. 4, which is a power-density plot for an aperture filled with low-ion-content water, showing the plane intersecting the axis of the central opening. This produces little attenuation of the dominant-mode field pattern. The pattern was obtained by scanning with the E-field probe as described above, and shows potential for

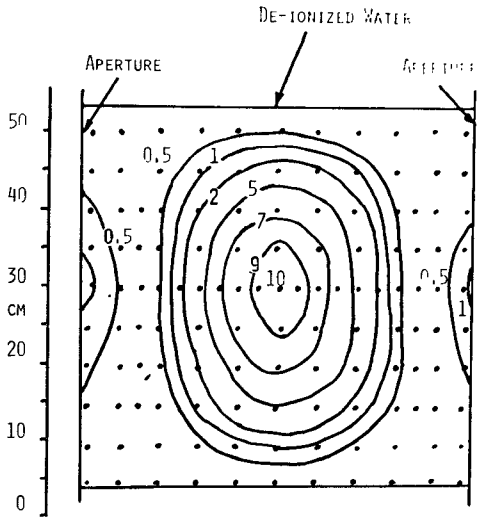


Fig. 4. Pattern of normalized power density along an axial central plane in a deionized water-filled aperture at 80 MHz (dots indicate data points from which curves were generated by interpolation).

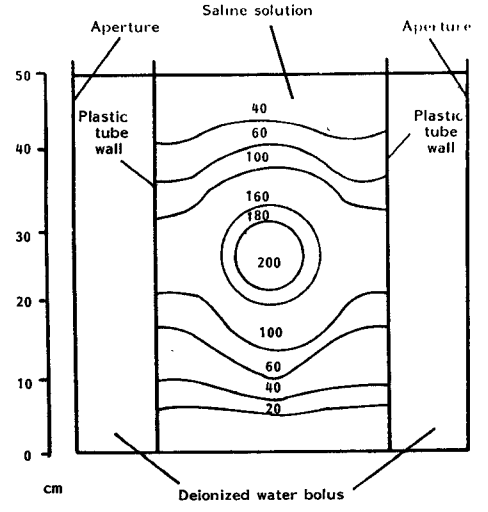


Fig. 5. Pattern of normalized power density at 74 MHz along an axial central plane in a tube having plastic walls 5 mm thick and an inside diameter of 32 cm; tube filled with saline solution having conductivity of 0.33 mhos/m, deionized water in the remaining 51-cm opening between opposing apertures; curves generated by interpolation from measurements made every 5 cm.

selective central heating. Good symmetry also exists in the full cross section (not shown).

Central heating may be achieved with this technique in other, nonmedical, applications for heating nonmetallic material having absorption losses less than those of the body, such as oils, oil shale, coal, various mineral compositions, and the like. In particular, the APA may be a unique means of achieving selective central heating of such solids. (Materials of lower permittivity would allow the use of higher frequencies, as would smaller masses; larger masses might require lower frequencies than usual.)

When the APA is loaded with a homogeneous fluid-filled cylinder having a cross section and dielectric properties which simulate those of the human body, the pattern is substantially modified. In such a case, the region of central

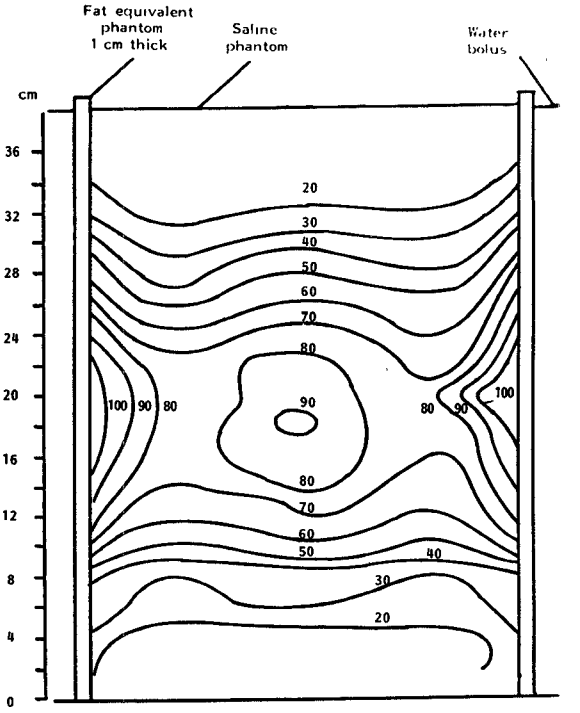


Fig. 6. Pattern of normalized power density at 80 MHz along central plane of major axis inside elliptical phantom with saline conductivity of 0.55 mhos/m; curves generated by interpolation from measurements made every 2 cm.

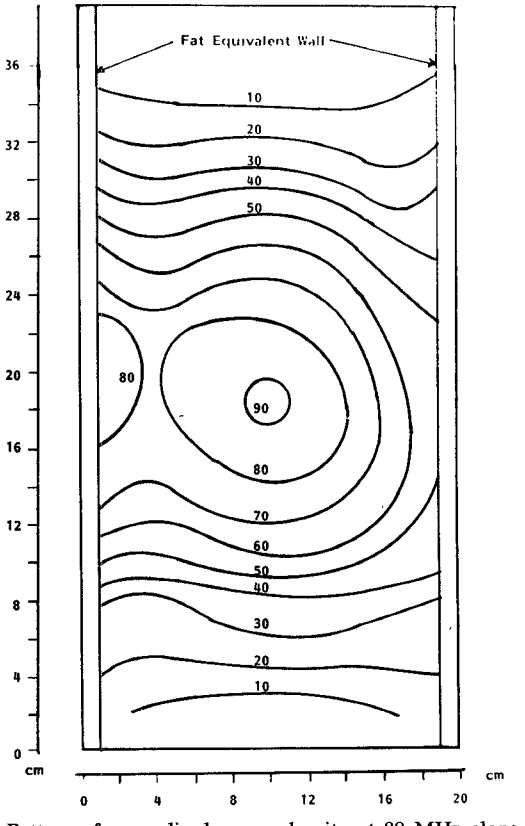


Fig. 7. Pattern of normalized power density at 80 MHz along central plane of minor axis inside elliptical phantom with saline conductivity of 0.55 mhos/m; curves generated by interpolation.

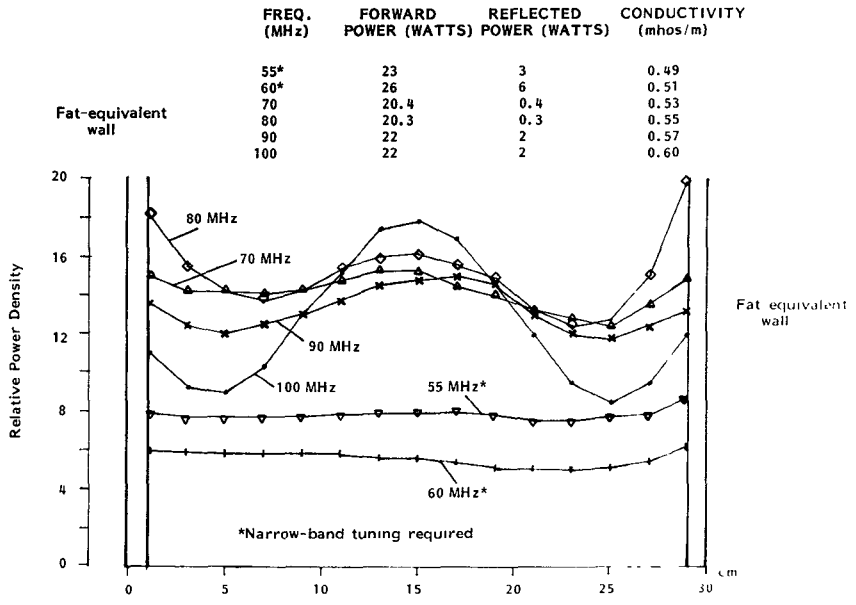


Fig. 8. Plot of relative power density versus distance across major axis cross section of elliptical phantom; salt content adjusted for each frequency; 15-cm position is central axis of phantom. NOTE: The phantom was slightly repositioned within the aperture to improve the pattern balance for each frequency.

focus shown in Fig. 4 becomes that of Fig. 5, which produces more uniform heating within the primary beam pattern throughout the cross section. A low-ion water bolus was used for coupling the radiated power to the cylinder.

As a general rule, the APA apertures are dielectrically loaded with deionized water having a dielectric constant of 78 and conductivity of 0.0022 mhos/m at 100 MHz and 25°C [13]. This actually causes a partial applicator mismatch, since the water loads the apertures to an impedance of about 25 Ω rather than the preferred 50 Ω. An improved broad-band match has been observed when apertures are filled with ethanol, which has a permittivity of 23.7 and a conductivity of 0.0083 mhos/m at 100 MHz [13]. This has proved to be true with both phantom and clinical testing. The heat pattern observed in similar testing with the ethanol-loaded apertures was found to be identical to that of Fig. 5.

An elliptical phantom formed of 1-cm-thick fat-equivalent material was also used to render a more accurate simulation of the patient interface to the ethanol-loaded apertures. The power density pattern along the plane of the major axis is shown in Fig. 6, and that of the minor axis in Fig. 7. Power density as measured at various frequencies along the center line of the major axis in fluid simulating losses of tissue at those respective frequencies is plotted in Fig. 8. Here, the conductivity is equal to two-thirds that of muscle for each frequency. Fig. 9 plots similar results along the minor elliptical axis of the phantom.

These data indicate that more uniform heating is achieved at the lower frequencies, while at higher frequencies localized central heating is increased. The greater levels which occur in the center at higher frequencies are caused in part by observable phase nulls along the outer tissue surfaces, and by power loss resulting from the narrow-band external

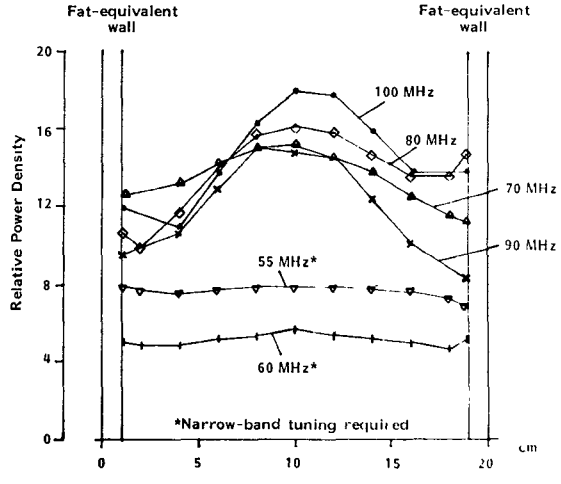


Fig. 9. Plot of relative power density versus distance across minor axis of elliptical phantom; test conditions and procedures same as those in Fig. 8; 10-cm position is central axis of phantom.

tuning, which is required to test levels of 55 and 60 MHz in the ethanol-loaded APA. (Use of a water bolus smaller than the usual size of approximately 46 cm makes such external tuning necessary.)

Mannequins of both male and female configuration have been constructed in order to make more accurate studies of the effects of external body contours on heating patterns. Initially, these were made of 3–4-mm-thick fiberglass; however, material this thick and having low dielectric constant and conductivity is not typical of actual human tissues. The fiberglass mannequin was later used as a mold to make a latex female mannequin with a 1.2-mm-thick latex layer inside a thin, rigid outer shell; the heating patterns achieved in the two were nearly identical.

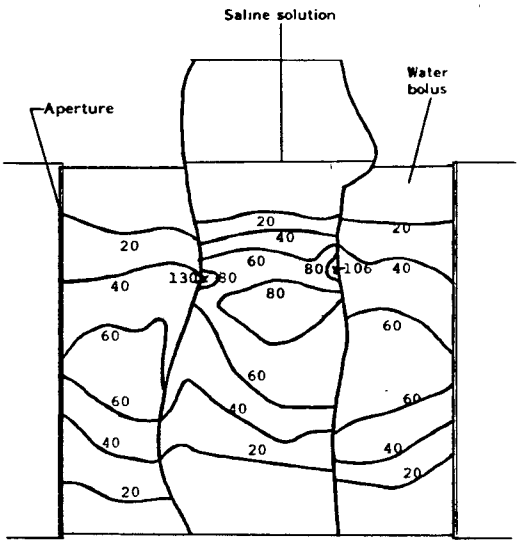


Fig. 10. Pattern of relative power density at 60 MHz for dorsoventral plane inside latex mannequin; saline conductivity 0.5 mhos/m; horizontal measurement points every 2.4 cm or less, vertical measurement points every 5 cm or less; contours interpolated between measurement points. Figure adapted from Turner, "Electromagnetic hyperthermia devices and methods."

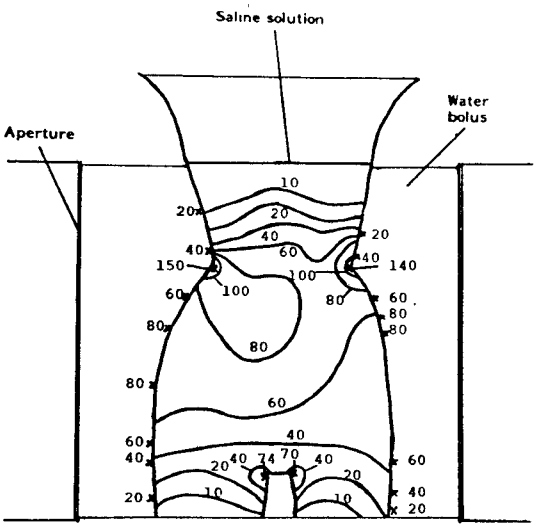


Fig. 11. Pattern of relative power density at 60 MHz for lateral plane inside latex-shell mannequin; saline conductivity 0.5 mhos/m; horizontal measurement points every 4 cm or less, vertical measurement points every 5 cm or less; contours interpolated between measurement points. Figure adapted from Turner, "Electromagnetic hyperthermia devices and methods."

Figs. 10 and 11 illustrate the relative power density contours in the dorsoventral and lateral planes, each passing through the central axis of the trunk. This test demonstrated that deep heating is possible even when diameters and surface contours change dramatically, although the pattern is shifted toward those regions having a smaller diameter. Some localized surface heating was observed, apparently where there was a horizontal surface interface (i.e., perpendicular to the dominant electric field). Locally increased fields occurred in the perhaps abnormally narrow waist of the female mannequin, and were also observed along the front of the inner upper thigh, where separation of the legs was more pronounced.

A review of some of the basic characteristics of tissue is helpful in explaining this phenomenon. At the VHF frequencies used by the Annular Phased Array, the magnitude of conduction currents $|J_C|$ is more dominant in muscle tissue than that of displacement currents $|J_D|$ by a ratio of usually 2 to 3 [9], as shown below

$$\frac{|J_C|}{|J_D|} = \frac{\sigma}{2\pi f \epsilon_0 \epsilon_r}$$

where $\sigma$ is the conductivity, $f$ is the frequency, $\epsilon_r$ is the relative permittivity, and $\epsilon_0$ is the free-space permittivity.

For muscle

$$\frac{|J_C|}{|J_D|} \text{ at 60 MHz} = 3.0$$

and

$$\frac{|J_C|}{|J_D|} \text{ at 100 MHz} = 2.23.$$

For bone and fat

$$\frac{|J_C|}{|J_D|} \text{ at 60 MHz} = 1.67$$

and

$$\frac{|J_C|}{|J_D|} \text{ at 100 MHz} = 1.84.$$

Thus, it is implied that currents induced in the body tend to follow the paths of more conductive tissue, being partially deflected along conductive parallel routes. Conductive currents are not supported by the deionized water in the external bolus, which therefore leaves only the weaker displacement currents in this area.

Strong quasi-static or inductive mutual coupling may be expected among currents within zones having a diameter less than $\lambda_m/\pi$, where $\lambda_m$ is the wavelength within the medium. In this quasi-static or induction zone, currents can be deflected by nonconductive and low-dielectric perpendicular interfaces, and they may also densify within more conductive paths in the same zone. This may be why increased heating occurred in the mannequin's waist as the induced currents above and below this region deflect inward with the surface contour, thus producing a localized "hot spot."

The area of the mannequin's waist was carefully scanned with E-field probes, and the hot zone was found to exist only within the outer 1 to 2 cm of conductive tissues. This was confirmed by embedding open-celled dielectric mesh in a cross section of the mannequin's trunk and placing temperature probes in this region, particularly at the point of maximum detected field. An RF power level of 2000 W was repeatedly applied for one-min periods. The heating in the small surface concavity of the mannequin's waist averaged a 2.0°C rise, as compared with a 0.9°C rise in phantom material in the center of the trunk. E-field scanning of these zones indicated that a difference of 2.23 was to be expected, and the observed comparison was 2.22. Therefore, the E-field probe's prediction of measured localization of heating is obviously valid.

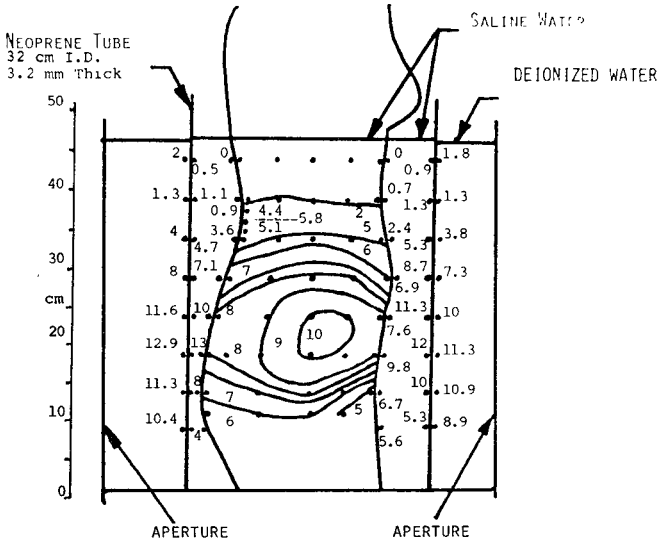


Fig. 12. Pattern of relative power density at 60 MHz for dorsoventral plane inside latex-shell mannequin; inner diameter 32 cm; both mannequin and neoprene tube saline solution-filled; conductivity 0.5 mhos/m; dots indicate data points from which contours were generated by interpolation; external levels also shown.

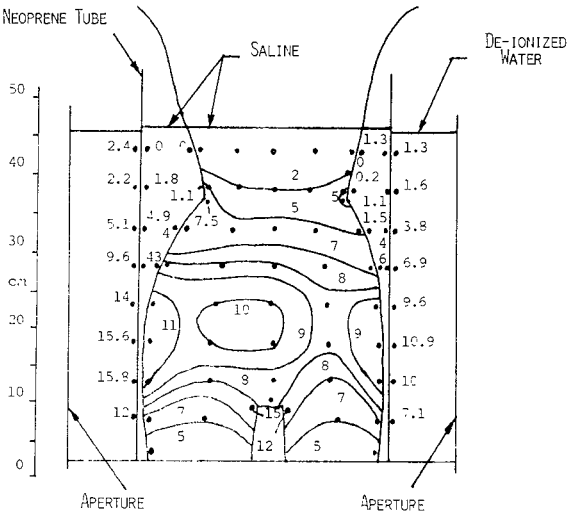


Fig. 13. Pattern of relative power density at 60 MHz for lateral plane inside latex-shell mannequin; inner diameter 32 cm; both mannequin and neoprene tube saline solution-filled; conductivity 0.5 mhos/m; dots indicate data points from which contours were generated by interpolation; external levels also shown.

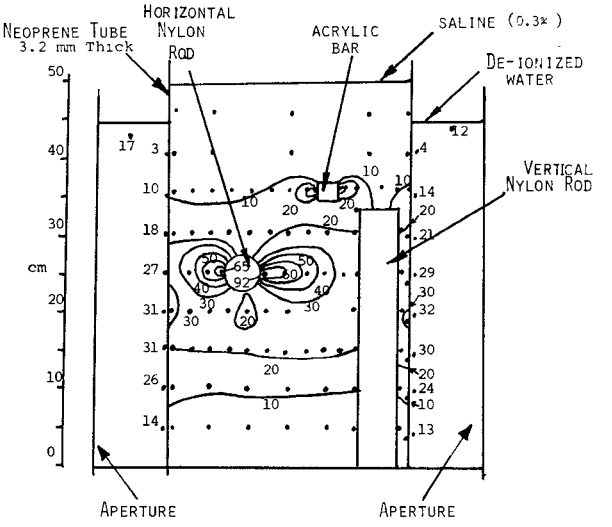


Fig. 14. Pattern of relative mean-squared electric field at 60 MHz (proportional to power density assuming effective medium impedance is constant) inside saline solution-filled neoprene tube; saline conductivity 0.4 mhos/m; long dielectric bars and rods inserted into central field; direction of E-field is vertical; dots indicate data points from which contours were generated by interpolation; external levels also shown.

In order to demonstrate the influence of body contours on the internal heating pattern, the setup of Figs. 10 and 11 was duplicated, except that the mannequin was placed inside a 0.3-percent saline solution-filled neoprene cylinder having walls 3.2 mm thick and a diameter of 32 cm. The resulting relative power density patterns are shown in Figs. 12 and 13. These figures illustrate that the potential for localized waist heating noted earlier was greatly suppressed. The deep pattern also shifted and became more axially symmetrical and centered within the width of the water bolus. However, the localized heating along the inner thigh was not reduced by the presence of the saline solution around the legs of the mannequin. (Localized "hot spots" in this area have occasionally been observed in patient treatments, but they have generally been lowered to acceptable levels by displacing the bolus from the thighs with low-density foam or by increasing surface cooling over the area with water-filled cooling pads.) Preliminary testing has indicated that a small sheet of metal 6 cm square can neutralize these intense superficial fields if it is placed 2–8 mm away from the surface of the mannequin's thighs. The practical application of this method to clinical use has not yet been determined.

The trunk of the human body is composed of many different tissue types. In general, all high-water tissues like muscle, lung, blood, and vital organs have similar permittivity and conductivity [8]. Bone and fat contain less water and have significantly lower permittivity and conductivity, and these parameters are even lower in air-filled regions such as the major bronchi, stomach, and large intestine.

As a means of better understanding the interaction of such diversified tissues with electric fields, nylon rods and acrylic bars were submerged in a saline solution-filled 3.2-mm-thick neoprene tube, the permittivity of which was about 5. This configuration and the resulting observations of the field are shown in Fig. 14. As was stated earlier, the fields within the heating region change in a smooth, continuous manner even near different tissue interfaces, which are large in comparison to a wavelength and parallel to the electric field. In this figure, the dominant E-field is vertical, and along the plotted observation points the field becomes more intense at the sides of the cross sections of the small bar and rod, which are parallel to the field, although it weakens along the perpendicular surfaces. This phenomenon illustrates a fundamental principle of Maxwell's Laws dealing with the interaction of electric fields which are perpendicular to different dielectric surfaces.

It should be noted, however, that little effect on the rod in line with the E-field is observed; this may depend on the

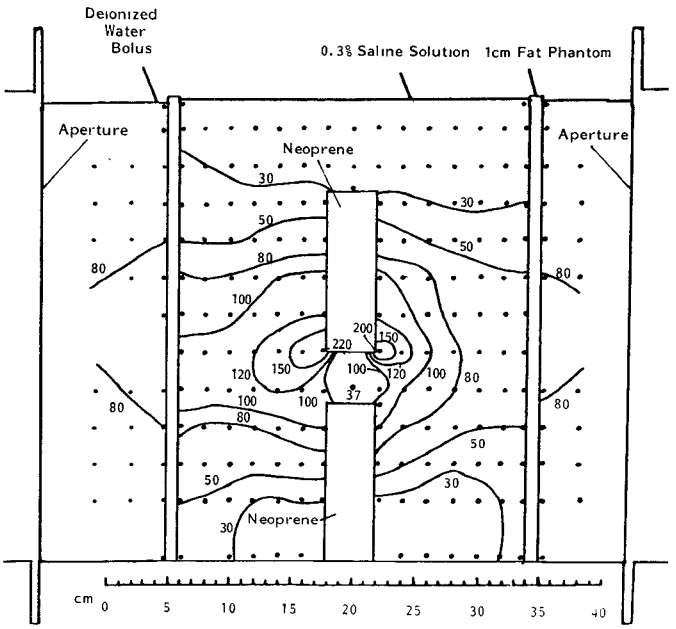


Fig. 15. Pattern of relative mean-squared electric field at 80 MHz (proportional to power density assuming effective medium impedance is constant) inside saline solution-filled elliptical phantom having 1-cm-thick walls of fat-equivalent phantom; saline conductivity 0.4 mhos/m; two neoprene bars, each 13 cm long and 4 cm square, inserted 4 cm apart in saline solution; major central axial plane shown, minor axis 18 cm across saline solution; dots indicate data points from which contours were generated by interpolation.

size of the rod as compared to the tissue wavelength, which is about 41 cm. Such a rod could be considered a model of the spine, although the relative permittivity of nylon and acrylic, i.e., 2.5 to 3, is much lower than that of bone and fat, which is typically 7 to 12 at the 55–110-MHz frequencies of the APA. Therefore, the interaction observed here produces a much greater effect than would be expected between muscle and bone.

The interaction of two square neoprene bars, each 4× 4 cm, is shown in Fig. 15. These bars were spaced 4 cm apart within an elliptical phantom having 1-cm-thick walls of fat-simulating phantom. The major axis scan is illustrated here; the elliptical minor axis is 18 cm across the inside of the phantom wall. The bars approximately simulate a bone which has undergone a high-water tumor ingress. As the figure shows, a tumor in such a location may be shielded from substantial heating by the field interaction of bone and tumor. Again, the field is substantially weaker along surfaces perpendicular to the E-field, with localized increases occurring near the edges parallel to the field. Such interaction likely occurs in regions where bones are perpendicular to the dominant E-field; therefore, local-applicator hyperthermia treatments of the chest, for example, may be better administered by orienting the E-field of the applicator in line with the underlying ribs to reduce local hot spots which could otherwise cause the patient unnecessary discomfort. (Selective heating of tissue around the ribs has not been clinically observed with the APA; however, this may be due to the surface cooling produced by the APA water bolus.)

## IV. Conclusions

The Annular Phased Array technique is capable of producing central heating in the trunk of the human body; however, the heating pattern produced will be influenced by body surface contours, as well as internal structures which have varying permittivities and conductivities.

Thin-walled phantom-filled mannequins, elliptical phantoms lined with artificial fat, and cylindrical neoprene phantoms have all been experimentally used to demonstrate the ability of the APA to direct heating power to the center of a tissue mass. Results of such testing demonstrate that more uniform central heating is achieved at the lower frequencies, 55–70 MHz, while at frequencies above this level, more centrally focused heating is obtained. It has been found, however, that the decreased depth of penetration achieved with frequencies over 200 MHz greatly reduces the efficacy of heating in the trunk of the body. A numerical solution which shows little central heating with a 433-MHz array has been previously reported [14].

The demonstrated effect of variations in anatomical configurations suggests that three-dimensional numerical methods which take into account the overall interaction of the body with electromagnetic fields are required to model and accurately predict heating patterns. An exact solution of this type is perhaps impossible to achieve at the present time, although it may be feasible to solve for a coarse block model with blocks less than $\lambda_m/\pi$ across and then to apply quasi-stationary methods to account for local effects of the tissues on conduction and displacement currents.

## References

[1] P. F. Turner, "Deep heating of cylindrical or elliptical tissue masses," presented at the Third Annual Symp. Cancer Therapy by Hyperthermia, Drugs, and Radiation, June 1980, NCI Monograph No. 61.

[2] _____, "Regional hyperthermia with an annular phased array," *IEEE Trans. Biomed. Eng.*, Special Issue on Hyperthermia, vol. BME-31, Jan. 1984.

[3] F. A. Gibbs, Jr., "Heating patterns in large cylindrical phantoms and pig thorax and abdomen using a 2 kilowatt, 55–100 MHz phased annular array applicator," presented at the 22nd Meeting of the American Society of Therapeutic Radiologists, Dallas, TX, Oct. 25, 1980.

[4] _____, "Clinical evaluation of a microwave/radiofrequency system (BSD Medical Corporation) for induction of local and regional hyperthermia," *J. Microwave Power*, vol. 16, no. 2, pp. 185–192, 1981.

[5] M. D. Sapozink, F. A. Gibbs, Jr., T. S. Sandhu, K. S. Settles, and J. R. Stewart, "Regional hyperthermia in the treatment of clinically advanced deep-seated malignancy: Results of a pilot study employing an annular phased array applicator system," presented at the 31st Meeting of the Radiation Research Society of the North American Hyperthermia Group, San Antonio, TX, Feb. 28, 1983.

[6] M. Iskander, P. F. Turner, J. B. DuBow, and J. Kao, "Two-dimensional technique to calculate the EM power deposition pattern in the human body," *J. Microwave Power*, vol. 17, no. 3, pp. 175–185, 1982.

[7] P. F. Turner, "Electromagnetic hyperthermia devices and methods," thesis submitted to the University of Utah for M.S.E.E., June 1983, pp. 140–160 (available from author).

[8] C. H. Durney *et al.*, Eds., *Radiofrequency Radiation Dosimetry Handbook*, 2nd ed. University of Utah Electrical Engineering and Bioengineering Departments, May 1978.

[9] M. Iskander, "Physical aspects and methods of hyperthermia pro-

duction by RF currents and microwaves," AAPM Summer School at Dartmouth College, Aug. 1981.
[10] P. F. Turner and O. P. Gandhi, U.S. Patent 4 271 848, June 9, 1981.
[11] P. F. Turner, "Electromagnetic Hyperthermia Devices and Methods," pp. 135–139.
[12] A. W. Guy *et al.*, "Electromagnetic power desposition in man exposed to high-frequency fields and the associated thermal and physiologic consequences," NTIS, 5285 Port Royal Road, Springfield, VA 22151, 1973.
[13] R. F. Harrington, *Time-Harmonic Electromagnetic Fields*. New York: McGraw-Hill, 1961, p. 455.
[14] P. F. Turner, "Electromagnetic hyperthermia devices and methods," p. 124.

**Paul F. Turner** was born in Salt Lake City, UT, on April 19, 1947. He received the B.S.E.E. degree in 1971 and the M.S.E.E. degree in 1983, both from the University of Utah. He initially specialized in microwave communications and antenna design for defense systems.

In August of 1978, he changed employment to BSD Medical Corporation. Since that time he has devoted full time to the development and design of microwave and RF applicators and methods for the purpose of hyperthermic cancer treatment. He has obtained five patents and several patents are pending related to his work.

# Microwave-Induced Post-Exposure Hyperthermia: Involvement of Endogenous Opioids and Serotonin

HENRY LAI, AKIRA HORITA, C. K. CHOU, MEMBER, IEEE, AND A. W. GUY, FELLOW, IEEE

*Abstract*—**Acute exposure to pulsed microwaves (2450 MHz, 1 mW/cm$^2$, SAR 0.6 W/kg, 2-$\mu$s pulses, 500 pulses/s) induces a transient post-exposure hyperthermia in the rat. The hyperthermia was attenuated by treatment with either the narcotic antagonist naltrexone or one of the serotonin antagonists cinanserin, cyproheptadine, or metergoline. It was not affected, however, by treatment with the peripheral serotonin antagonist xylamidine nor the dopamine antagonist haloperidol. It thus appears that both endogenous opioids and central serotonin are involved. It is proposed that pulsed microwaves activate endogenous opioid systems, and that they in turn activate a serotonergic mechanism that induces the rise in body temperature.**

## I. Introduction

IN PREVIOUS RESEARCH, we concluded that acute exposure to low-level, pulsed microwaves activates endogenous opioids in the rat on the basis of our findings that: 1) microwaves induced a post-exposure hyperthermia that was blockable by the narcotic antagonist naloxone [1]; 2) microwaves enhanced amphetamine-induced hyperthermia, an effect that was also blockable by naloxone [2]; 3) microwaves enhanced morphine-induced catalepsy [3]; and 4) microwaves attenuated the naloxone-induced withdrawal syndrome in morphine-dependent rats [1].

Manuscript received October 12, 1983; revised March 7, 1984. This work was supported in part by the Office of Naval Research under Contract N00014-80-C-0354.

The authors are with the Departments of Pharmacology, Psychiatry, and Behavioral Sciences, and the Center for Bioengineering, University of Washington School of Medicine, Seattle, WA 98195.

The post-exposure hyperthermia was a most consistent response of rats to exposure to pulsed microwaves. In further experiments we found this effect to be classically conditionable to cues in the exposure environment and the conditioned response to be also attenuable by naloxone, suggesting the involvement of endogenous opioids [1], [2]. In this paper, we report further experiments elucidating the neural mechanisms underlying the post-exposure hyperthermia. They showed that serotonin in the central nervous system plays an important role in mediating the effect.

## II. Methods and Materials

### *Animals*

Male Sprague–Dawley rats (250–300 g), obtained from Tyler Lab., Bellevue, WA, were used. They were housed in a temperature-controlled vivarium (22°C) maintained at a 12-h light–dark cycle (lights on between 8 A.M. and 8 P.M.). They were housed four to a cage and provided with food and water *ad libitum*. Each animal was used once in the experiments.

### *Drugs and Controls for Drug Injection*

Drugs used consisted of the serotonin antagonists cinanserin (Squibb & Sons Inc., New Brunswick, NJ), cyproheptadine (Merck, Sharp & Dohme, West Point, PA), and metergoline (Soc. Pharmaceutici, Milano, Italy); a dopamine antagonist haloperidol (Haldol; McNeilab Inc.,

0018-9480/84/0800-0882$01.00 ©1984 IEEE